Supplementary Material for: Densities, Viscosities, and Diffusivities of Loaded and Unloaded Aqueous CO_2/H_2S/MDEA Mixtures: A Molecular Dynamics Simulation Study

H. Mert Polat[a], Casper van der Geest[a], Frédérick de Meyer[b,c], Céline Houriez[c], Thijs J. H. Vlugt[a], Othonas A. Moultos[a,*]

[a] *Engineering Thermodynamics, Process & Energy Department, Faculty of Mechanical Engineering, Delft University of Technology, Leeghwaterstraat 39, Delft 2628CB, The Netherlands*

[b] *CO_2 and Sustainability R&D Program, Gas & Low Carbon Entity, OneTech, TotalEnergies S.E., 92078 Paris, France*

[c] *Mines Paris, PSL University, Center for Thermodynamics of Processes (CTP), 77300 Fontainebleau, France*

[*] Corresponding author

Email address: o.moultos@tudelft.nl (Othonas A. Moultos)

Preprint submitted to Fluid Phase Equilibria *July 22, 2023*

The following items are presented in this Supplementary Material:

- Functional forms of the Arrhenius, Speedy-Angell and Vogel-Tamann-Fulcher (VTF) equations (section S1),
- Force field parameters used in MD simulations (Tables S1–S22),
- Compositions of the simulation boxes used in the MD simulations of CO_2 and H_2S-loaded aqueous MDEA simulations (Tables S23 and S24),
- Speedy-Angell and VTF fit parameters for the self-diffusivities D_{CO_2} and D_{H_2S} in aqueous MDEA solutions (Tables S25–S28),
- Computed and experimental [1, 2] self-diffusivities D_{CO_2} and D_{H_2S} in pure water as a function of temperature (Figure S3),
- Dihedral potential energy as a function of dihedral angle for the N–C–C–O dihedral in MDEA for the dihedral parameters from Cornell et al. [3] and Orozco et al. [4] (Figure S4),
- Computed and experimental [1] densities of aqueous MDEA solutions as a function of temperature and MDEA concentration with $\chi^q_{MDEA} = 1$ (Figure S5),
- Comparison between the self-diffusivities of MDEA in 50 wt.% MDEA/water solutions and MEA in 30 wt.% MEA/water solutions as a function of temperature (Figure S6),
- Comparison between the self-diffusivities D_{CO_2} and D_{H_2S} in aqueous MDEA solutions and 30 wt.% MEA/water solutions (Figure S7),
- Computed values of the self-diffusivities D_{CO_2} and D_{H_2S} as a function of temperature and MDEA concentration, and the fits to the Arrhenius, Speedy-Angell and VTF equations, respectively (Figures S8, S9, and S10).

S1. Arrhenius, Speedy-Angell Power, and Vogel-Tamann-Fulcher Equations

We fit the values of D_{CO_2} and D_{H_2S} in aqueous MDEA solutions to the Arrhenius equation, the Speedy-Angell power equation [5], and the Vogel-Tamann-Fulcher (VTF) equation [6]. The Arrhenius equation equals:

$$D_{\text{self}} = D_0 \exp\left[-\frac{E_A}{RT}\right] \tag{S1}$$

where D_{self} is the self-diffusion coefficient, D_0 is the pre-exponential factor, T is the absolute temperature, R is the ideal gas constant, and E_A is the activation energy for diffusion. The Speedy-Angell power equation equals:

$$D_{\text{self}} = D_0 \left(\frac{T}{T_s} - 1\right)^m \tag{S2}$$

where T_s is the singularity temperature and m is a fit parameter. We also fit the values of D_{CO_2} and D_{H_2S} to the VTF equation using:

$$D_{\text{self}} = \exp\left[\frac{-\alpha}{T - \beta} - \gamma\right] \tag{S3}$$

where α, β, and γ are fit parameters.

Table S1: The atom types and coordinates of the TraPPE [7] CO_2 molecule.

Atom type	x / [Å]	y / [Å]	z / [Å]
C	1.16	0.00	0.00
O	0.00	0.00	0.00
O	2.32	0.00	0.00

Table S2: Force field parameters for carbon dioxide. The TraPPE [7] force field was used for carbon dioxide.

Atom	ϵ/k_B / [K]	σ / [Å]	q / [e^-]
O	79.0	3.05	-0.35
C	27.0	2.80	0.70

Table S3: The atom types and coordinates of the TraPPE [8] H_2S molecule.

Atom type	x / [Å]	y / [Å]	z / [Å]
S	0.0000000	0.0000000	0.0000000
H	1.3400000	0.0000000	0.0000000
H	-0.0467526	1.3391826	0.0000000

Table S4: Force field parameters for hydrogen sulfide. The TraPPE [8] force field was used for hydrogen sulfide.

Atom	ϵ/k_B / [K]	σ / [Å]	q / [e^-]
S	125.0	3.60	-0.28
H	50.0	2.50	0.14

Table S5: The atom types and coordinates of the TIP4P/2005 [9] water molecule. The atom type M represents the dummy charge site in the TIP4P/2005 force field.

Atom type	x / [Å]	y / [Å]	z / [Å]
O	0.00000000	0.00000000	0.00000000
H	-0.75695033	0.58588228	0.00000000
H	0.75695033	0.58588228	0.00000000
M	0.00000000	0.15000000	0.00000000

Table S6: Force field parameters for water. The TIP4P/2005 [9] force field was used for water.

Atom	ϵ/k_B / [K]	σ / [Å]	q / [e^-]
O	81.899	3.16435	0.00000
H	0.0000	0.00000	0.52422
M	0.0000	0.00000	-1.04844

Table S7: Non-bonded interaction parameters between CO_2 and water. The optimized potential developed by Orozco et al. [10] was used.

Atoms	ϵ/k_B / [K]	σ / [Å]
$O_{CO_2} - O_{H_2O}$	79.14	3.058
$C_{CO_2} - O_{H_2O}$	53.04	3.052

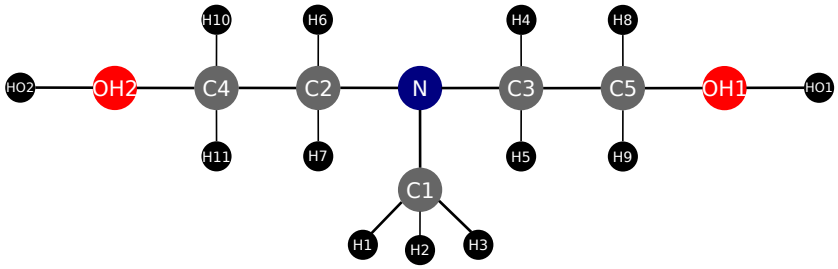

Figure S1: Schematic representation showing the atom type designation of MDEA. Color code: black: hydrogen; blue: nitrogen; red: oxygen; grey: carbon.

Table S8: Intermolecular force field parameters for MDEA. The OPLS-AA force field [11, 12] with point charges computed by quantum chemical calculations (MP2/6-311+G(2d,2p)) was used for MDEA. The point charges listed in this table are unscaled charges, i.e. $\chi^q_{\mathrm{MDEA}} = 1.0$. The tabulated point charges sum up to zero. As explained in the main text, in our simulations, these point charges are scaled by $\chi^q_{\mathrm{MDEA}} = 0.9$. The atom labels are defined in Fig. S1.

Atom	ϵ/k_{B} / [K]	σ / [Å]	q / [e^-]
N	85.47	3.30	-0.63525
C1	33.18	3.50	-0.26080
C2	33.18	3.50	-0.10893
C3	33.18	3.50	-0.11385
C4	33.18	3.50	0.06446
C5	33.18	3.50	0.06972
OH1	85.47	3.12	-0.78207
OH2	85.47	3.12	-0.77757
H1	15.08	2.50	0.16784
H2	15.08	2.50	0.16269
H3	15.08	2.50	0.14238
H4	15.08	2.50	0.17381
H5	15.08	2.50	0.15235
H6	15.08	2.50	0.17490
H7	15.08	2.50	0.14150
H8	7.54	2.50	0.12994
H9	7.54	2.50	0.12320
H10	7.54	2.50	0.12901
H11	7.54	2.50	0.12130
HO1	0.50	1.00	0.46226
HO2	0.50	1.00	0.46311

Table S9: Harmonic bond stretching potential parameters for MDEA. The OPLS-AA [11, 12] force field is used for MDEA. To compute the bonding potentials, we use $U_{\text{bond}} = K(r - r_0)^2$ where K is the bond coefficient, r is the distance between two atoms, and r_0 is the equilibrium distance between two atoms. The atom labels are defined in Fig. S1.

Bond	r_0 / [Å]	K/k_{B} / [K Å^{-2}]
C–C	1.529	134735.7
C–H	1.090	170933.4
C–N	1.448	192048.7
C–O	1.410	160878.5
O–H	0.960	278018.2

Table S10: Harmonic bond bending angle potential parameters for MDEA. The OPLS-AA [11, 12] force field is used for MDEA. To compute the angle potentials, we use $U_{\text{angle}} = K(\theta - \theta_0)^2$ where K is the bending strength, θ is the bending angle between three atoms, and θ_0 is the equilibrium bending angle. The atom labels are defined in Fig. S1.

Angle	θ_0 / [°]	K/k_{B} / [K]
C–C–H	110.70	18852.9
C–C–N	109.47	28254.3
C–C–O	109.50	25137.3
C–O–H	108.50	27651.0
H–C–H	107.80	16590.6
H–C–N	109.50	17596.1
H–C–O	109.50	25137.3

Table S11: OPLS-AA dihedral potential parameters for MDEA. The OPLS-AA [11, 12] force field is used for the dihedrals in MDEA, except for the N–C–C–O dihedral. For the N–C–C–O dihedral, we either use the parameters reported by Cornell et al. [3] or Orozco et al. [4]. To compute the dihedral potential for the dihedrals in this table, we use $U_{\text{dihedral}} = \frac{1}{2}K_1\left[1 + \cos(\phi)\right] + \frac{1}{2}K_2\left[1 - \cos(2\phi)\right] + \frac{1}{2}K_3\left[1 + \cos(3\phi)\right] + \frac{1}{2}K_4\left[1 - \cos(4\phi)\right]$ where $K_1..K_4$ are the dihedral coefficients and ϕ is the dihedral angle. The values of K_4 are 0 for all dihedrals listed in this table. The atom labels are defined in Fig. S1.

Dihedral	K_1/k_{B} / [K]	K_2/k_{B} / [K]	K_3/k_{B} / [K]
H–C–N–C [11, 12]	0.00	0.00	281.54
C–N–C–C [11, 12]	209.14	-64.35	349.41
C–C–O–H [11, 12]	-178.98	-87.48	247.35
N–C–C–O [3]	0.00	0.00	1407.69

Table S12: The optimized parameters for N–C–C–O dihedral from Orozco et al. [4]. All energies in this table are divided by the Boltzmann constant k_B and reported in units of K. To compute the dihedral potential for the N–C–C–O dihedral with the parameters in this table, we use $U_{\text{dihedral}} = \sum_{i=1,9} \left[a_i cos^{i-1}(\phi)\right]$ where $a_1..a_9$ are the dihedral coefficients and ϕ is the dihedral angle. The atom labels are defined in Fig. S1.

Dihedral	a_1/k_B	a_2/k_B	a_3/k_B	a_4/k_B	a_5/k_B	a_6/k_B	a_7/k_B	a_8/k_B	a_9/k_B
N–C–C–O	57.00	5889.99	1231.11	-9428.99	-6584.23	14567.26	6614.81	-11345.20	2511.20

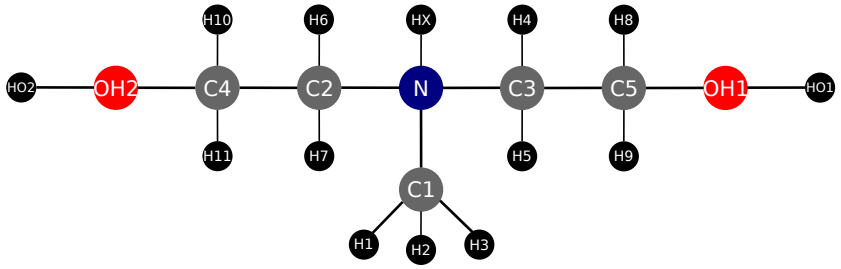

Figure S2: Schematic representation showing atom type designations of $MDEAH^+$. Color code: black: hydrogen; blue: nitrogen; red: oxygen; grey: carbon.

Table S13: Intermolecular force field parameters for $MDEAH^+$. The OPLS-AA force field [11, 12] with point charges computed by quantum chemical calculations (MP2/6-311+G(2d,2p)) was used for $MDEAH^+$. The point charges listed in this table are unscaled charges, i.e. $\chi^q_{\mathrm{MDEAH^+}} = 1.0$. The tabulated point charges sum up to exactly 1. As explained in the main text, in our simulations, these point charges are scaled by 0.90 or 0.75. The atom labels are defined in Fig. S2.

Atom	ϵ/k_B / [K]	σ / [Å]	q / [e^-]
N	85.47	3.25	-0.47548
C1	33.18	3.50	-0.30317
C2	33.18	3.50	-0.14067
C3	33.18	3.50	-0.13852
C4	33.18	3.50	-0.00517
C5	33.18	3.50	-0.00620
OH1	85.47	3.12	-0.76945
OH2	85.47	3.12	-0.76864
H1	15.08	2.50	0.21511
H2	15.08	2.50	0.20877
H3	15.08	2.50	0.20350
H4	15.08	2.50	0.20965
H5	15.08	2.50	0.20554
H6	15.08	2.50	0.20990
H7	15.08	2.50	0.20690
H8	15.08	2.50	0.18279
H9	15.08	2.50	0.15767
H10	15.08	2.50	0.18284
H11	15.08	2.50	0.15725
HO1	1.00	1.00	0.49508
HO2	1.00	1.00	0.49556
HX	1.00	1.00	0.47674

Table S14: Harmonic bond stretching potential parameters for $MDEAH^+$. The OPLS-AA [11, 12] force field is used for $MDEAH^+$. To compute the bonding potentials, we use $U_{\text{bond}} = K(r - r_0)^2$ where K is the bond coefficient, r is the distance between two atoms, and r_0 is the equilibrium distance between two atoms. The atom labels are defined in Fig. S2.

Bond	r_0 / [Å]	K/k_{B} / [K Å^{-2}]
C–C	1.529	134735.7
C–H	1.090	170933.4
C–N	1.471	184507.5
C–O	1.410	160878.5
O–H	0.945	278018.2
N–H	1.01	218191.5

Table S15: Harmonic bond bending angle potential parameters for $MDEAH^+$. The OPLS-AA [11, 12] force field is used for $MDEAH^+$. To compute the angle potentials, we use $U_{\text{angle}} = K(\theta - \theta_0)^2$ where K is the bending strength, θ is the bending angle between three atoms, and θ_0 is the equilibrium bending angle. The atom labels are defined in Fig. S2.

Angle	θ_0 / [°]	K/k_{B} / [K]
C–C–H	110.70	18852.9
C–C–N	111.20	40219.6
C–C–O	109.50	25137.3
C–O–H	108.50	27651.0
C–N–C	113.00	25137.3
C–N–H	107.64	16163.3
H–C–H	107.80	16590.6
H–C–N	109.50	17596.1
H–C–O	109.50	17596.1

Table S16: OPLS-AA dihedral potential parameters for $MDEAH^+$. The OPLS-AA [11, 12] force field is used for the dihedrals in $MDEAH^+$ except for the N–C–C–O dihedral. For the N–C–C–O dihedral, we used the parameters reported by Orozco et al. [4] (Table S12). To compute the dihedral potential for the dihedrals in this table, we use $U_{\text{dihedral}} = \frac{1}{2}K_1\left[1+\cos(\phi)\right]+\frac{1}{2}K_2\left[1-\cos(2\phi)\right]+\frac{1}{2}K_3\left[1+\cos(3\phi)\right]+\frac{1}{2}K_4\left[1-\cos(4\phi)\right]$ where $K_1..K_4$ are the dihedral coefficients and ϕ is the dihedral angle. The values of K_4 are 0 for all dihedrals listed in this table. The atom labels are defined in Fig. S2.

Dihedral	K_1/k_B / [K]	K_2/k_B / [K]	K_3/k_B / [K]
C–C–O–H	-178.98	-87.48	247.35
C–N–C–C	722.95	-62.34	132.72
H–C–N–C	0.00	0.00	151.83
N–C–C–H	0.00	0.00	193.05
H–C–N–H	0.00	0.00	131.22
H–C–O–H	0.00	0.00	176.97
H–C–C–O	0.00	0.00	235.28
H–N–C–C	0.00	0.00	174.45
H–C–C–H	0.00	0.00	150.82

Table S17: Intermolecular force field parameters for HCO_3^-. The OPLS-AA force field [11, 12] with point charges computed by quantum chemical calculations (MP2/6-311+G(2d,2p)) was used for HCO_3^-. The point charges listed in this table are unscaled charges, i.e. $\chi^q_{HCO_3^-} = 1.0$. The tabulated point charges sum up to exactly -1. As explained in the main text, in our simulations, these point charges are scaled by 0.90 or 0.75. The atom labels are as follows: C: carbon of HCO_3^-; O1: oxygen connected to carbon in HCO_3^-; O2: oxygen connected to carbon in HCO_3^-; OH: oxygen of OH group in HCO_3^-; HO: hydrogen of OH group in HCO_3^-.

Atom	ϵ/k_B / [K]	σ / [Å]	q / [e^-]
C	35.190	3.55	1.15070
O1	105.58	2.96	-0.90698
O2	105.58	2.96	-0.86222
OH	85.470	3.12	-0.83705
HO	1.0000	1.00	0.45555

Table S18: Harmonic bond stretching potential parameters for HCO_3^-. The OPLS-AA [11, 12] force field is used for HCO_3^-. To compute the bonding potentials, we use $U_{\text{bond}} = K(r - r_0)^2$ where K is the bond coefficient, r is the distance between two atoms, and r_0 is the equilibrium distance between two atoms. The atom labels are designated in the caption of Table S17.

Bond	r_0 / [Å]	K/k_{B} / [K Å^{-2}]
C–O	1.250	329800.9
C–OH	1.364	226235.4
OH-HO	0.945	278018.2

Table S19: Harmonic bond bending angle potential parameters for HCO_3^-. The OPLS-AA [11, 12] force field is used for HCO_3^-. To compute the angle potentials, we use $U_{\text{angle}} = K(\theta - \theta_0)^2$ where K is the bending strength, θ is the bending angle between three atoms, and θ_0 is the equilibrium bending angle. The atom labels are designated in the caption of Table S17.

Angle	θ_0 / [°]	K/k_{B} / [K]
O–C–OH	121	40219.6
O–C–O	126	40219.6
C–OH–HO	113	17596.1

Table S20: OPLS-AA dihedral potential parameters for HCO_3^-. The OPLS-AA [11, 12] force field is used for the dihedrals in HCO_3^-. To compute the dihedral potential for the dihedrals in this table, we use $U_{\text{dihedral}} = \frac{1}{2}K_1[1 + \cos(\phi)] + \frac{1}{2}K_2[1 - \cos(2\phi)] + \frac{1}{2}K_3[1 + \cos(3\phi)] + \frac{1}{2}K_4[1 - \cos(4\phi)]$ where $K_1..K_4$ are the dihedral coefficients and ϕ is the dihedral angle. The values of K_4 are 0 for all dihedrals listed in this table. The atom labels are designated in the caption of Table S17.

Dihedral	K_1/k_{B} / [K]	K_2/k_{B} / [K]	K_3/k_{B} / [K]
O–C–OH–HO	0.0	2765.1	0.0

Table S21: Intermolecular force field parameters for SH^-. The OPLS-AA force field [11, 12] with point charges computed by quantum chemical calculations (MP2/6-311+G(2d,2p)) was used for SH^-. The point charges listed in this table are unscaled charges, i.e. $\chi^q_{SH^-} = 1.0$. The tabulated point charges sum up to exactly -1. As explained in the main text, in our simulations, these point charges are scaled by 0.90 or 0.75.

Atom	ϵ/k_B / [K]	σ / [Å]	q / [e^-]
S	125.69	3.55	-1.04173
H	1.0000	1.00	0.04173

Table S22: Harmonic bond stretching potential parameters for SH^-. The OPLS-AA [11, 12] force field is used for SH^-. To compute the bonding potentials, we use $U_{bond} = K(r - r_0)^2$ where K is the bond coefficient, r is the distance between two atoms, and r_0 is the equilibrium distance between two atoms.

Bond	r_0 / [Å]	K/k_B / [K Å^{-2}]
S–H	1.351103	502745.3

Table S23: Number of MDEA, HCO_3^-, $MDEAH^+$, and water molecules in CO_2-loaded 50 wt.% MDEA/water solutions at 313 K as a function of CO_2 loading in the solution. To compute the self-diffusivities of CO_2, we also have two molecules of CO_2 in the solution. In these simulations, the point charges of MDEA are scaled by 0.9, and the point charges of $MDEAH^+$ and HCO_3^- are scaled by either 0.9 or 0.75. The point charges of CO_2 and water are not scaled. The average simulation box sizes are computed at 313 K and 1 bar.

CO_2 loading / [mol_{CO_2} mol^{-1}_{MDEA}]	0.01	0.1	0.5	1.0
N_{MDEA} (molar mass = 119.163 g mol^{-1})	150	205	153	29
$N_{HCO_3^-}$ (molar mass = 61.02 g mol^{-1})	1	21	148	272
N_{MDEAH^+} (molar mass = 120.17 g mol^{-1})	1	21	148	272
N_{H_2O} (molar mass = 18.02 g mol^{-1})	1000	1500	2000	2000
Average box size / [Å]	38.5	44.3	49.8	50.9

Table S24: Number of MDEA, SH^-, $MDEAH^+$, and water molecules in H_2S-loaded 50 wt.% MDEA/water solutions at 313 K as a function of H_2S loading in the solution. In these simulations, the point charges of MDEA are scaled by 0.9, and the point charges of $MDEAH^+$ and SH^- are scaled by either 0.9 or 0.75. To compute the self-diffusivities of H_2S, we also have two molecules of H_2S in the solution. The point charges of H_2S and water are not scaled. The average simulation box sizes are computed at 313 K and 1 bar.

H_2S loading / $[mol_{H_2S}\ mol^{-1}_{MDEA}]$	0.01	0.1	0.5	1.0
N_{MDEA} (molar mass = $119.163\,g\,mol^{-1}$)	224	203	156	48
N_{SH^-}(molar mass = $33.07\,g\,mol^{-1}$)	2	23	146	254
N_{MDEAH^+} (molar mass = $120.17\,g\,mol^{-1}$)	2	23	146	254
N_{H_2O} (molar mass = $18.02\,g\,mol^{-1}$)	1500	1500	2000	2000
Average box size / [Å]	44.0	44.2	49.3	49.9

Table S25: Speedy-Angell power equation [5] ($D_{self} = D_0 \left(\frac{T}{T_s} - 1\right)^m$) fit parameters ($D_0$, T_S and m) and coefficient of determinations (R^2) for the self diffusivity of CO_2 D_{CO_2} in aqueous MDEA solutions for different MDEA concentrations. The values of D_{CO_2} were fitted for a temperature range of 288–323 K.

MDEA concentration / [wt.%]	D_0 / $[m^2\,s^{-1}]$	T_S / [K]	m	R^2
10	3.07×10^{-28}	0.710	7.14	0.992
20	3.36×10^{-47}	0.045	9.84	0.999
30	1.30×10^{-8}	238.659	1.82	0.979
40	5.80×10^{-46}	0.155	10.98	0.984
50	4.31×10^{-9}	205.738	2.70	0.992

Table S26: Speedy-Angell power equation [5] ($D_{self} = D_0 \left(\frac{T}{T_s} - 1\right)^m$) fit parameters ($D_0$, T_S and m) and coefficient of determinations (R^2) for the self diffusivity of H_2S D_{H_2S} in aqueous MDEA solutions for different MDEA concentrations. The values of D_{H_2S} were fitted for a temperature range of 288–323 K.

MDEA concentration / [wt.%]	D_0 / $[m^2\,s^{-1}]$	T_S / [K]	m	R^2
10	7.78×10^{-9}	263.827	0.82	0.989
20	1.30×10^{-8}	252.324	1.49	0.991
30	7.27×10^{-9}	265.252	1.04	0.985
40	1.51×10^{-35}	0.537	9.32	0.989
50	4.34×10^{-9}	273.395	0.91	0.995

Table S27: Vogel-Tamann-Fulcher (VTF) equation [6] ($D_{\text{self}} = \exp\left[\frac{-\alpha}{T-\beta} - \gamma\right]$) fit parameters ($\alpha$, β, γ) and coefficient of determinations (R^2) for the self diffusivity of CO_2 D_{CO_2} in aqueous MDEA solutions for different MDEA concentrations. The values of D_{CO_2} were fitted for a temperature range of 288–323 K.

MDEA concentration / [wt.%]	α	β	γ	R^2
10	1.88×10^4	-5.92×10^2	-9.30×10^{-1}	0.992
20	9.02×10^5	-5.02×10^3	-1.49×10^2	0.999
30	3.67×10^2	1.91×10^2	1.73×10^1	0.979
40	3.01×10^8	-9.18×10^4	-3.25×10^3	0.988
50	1.14×10^3	1.01×10^2	1.57×10^1	0.992

Table S28: Vogel-Tamann-Fulcher (VTF) equation [6] ($D_{\text{self}} = \exp\left[\frac{-\alpha}{T-\beta} - \gamma\right]$) fit parameters ($\alpha$, β, γ) and coefficient of determinations (R^2) for the self diffusivity of H_2S D_{H_2S} in aqueous MDEA solutions for different MDEA concentrations. The values of D_{H_2S} were fitted for a temperature range of 288–323 K.

MDEA concentration / [wt.%]	α	β	γ	R^2
10	1.19×10^2	2.28×10^2	1.86×10^1	0.990
20	2.97×10^2	2.03×10^2	1.76×10^1	0.991
30	1.44×10^2	2.31×10^2	1.88×10^1	0.986
40	3.36×10^6	-1.02×10^4	-2.98×10^2	0.989
50	1.03×10^2	2.46×10^2	1.95×10^1	0.995

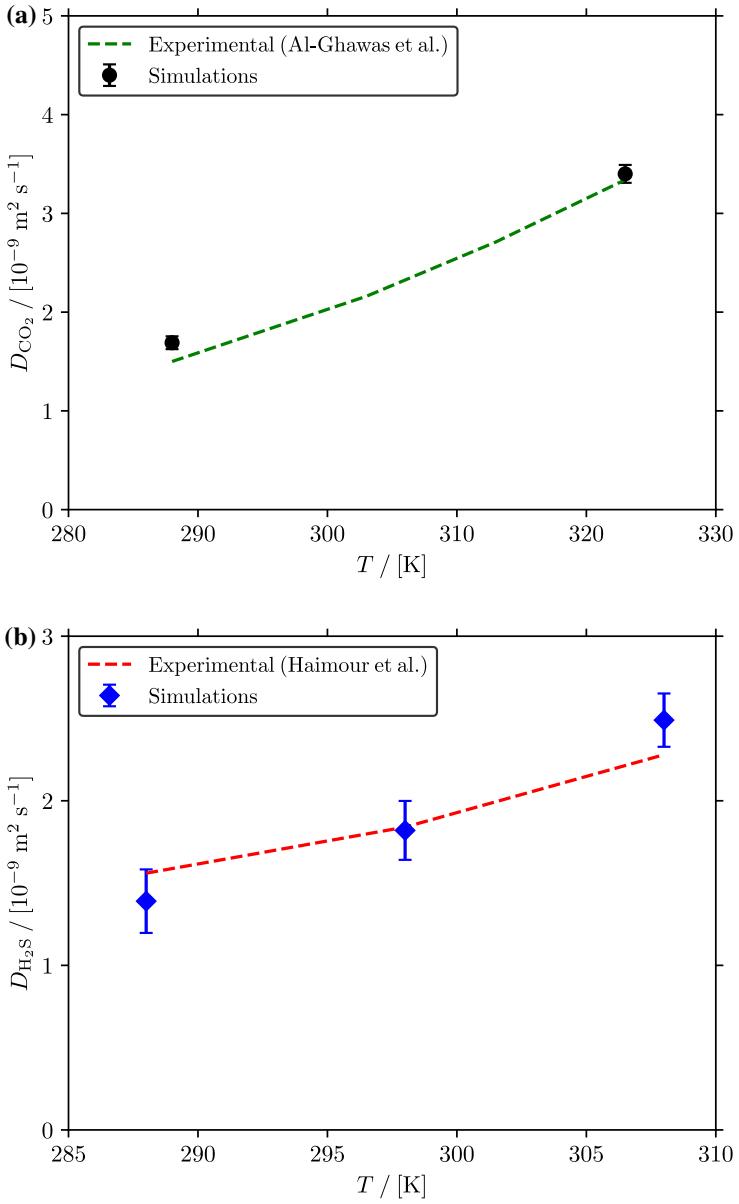

Figure S3: Computed and experimental [1, 2] self-diffusion coefficients of (a) CO_2 and (b) H_2S in pure water as a function of temperature at 1 bar. The self-diffusivities are corrected for finite-size effects using Eq. 1 of the main text. For CO_2 and H_2S, TraPPE [7, 8] force field is used while the TIP4P/2005 [9] force field is used for water (see Tables S1–S7).

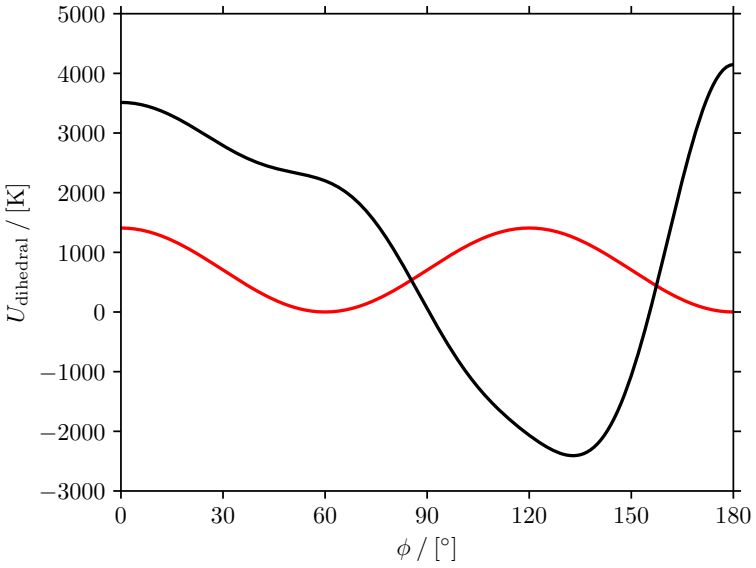

Figure S4: Dihedral potential energy as a function of dihedral angle for N–C–C–O dihedral in MDEA. The red curve represent the dihedral potential from Cornell et al. [3] (Table S11) while the black curve represent the dihedral potential from Orozco et al. [4] (Table S12).

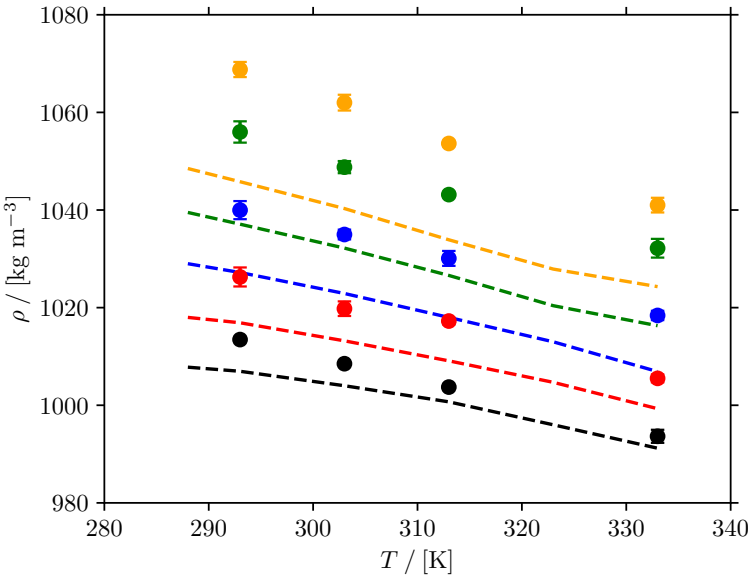

Figure S5: Computed and experimental [1] densities of aqueous MDEA solutions as a function of temperature at 1 bar. Note that the point charges of MDEA are not scaled, i.e. $\chi^q_{\mathrm{MDEA}} = 1$ and the parameters from Cornell et al. [3] are used for the N–C–C–O dihedral in MDEA. Dashed lines represent experimental results from Al-Ghawas et al. [1]. Color code: black: 10 wt.% MDEA/water; red: 20 wt.% MDEA/water; blue: 30 wt.% MDEA/water; green: 40 wt.% MDEA/water; orange: 50 wt.% MDEA/water.

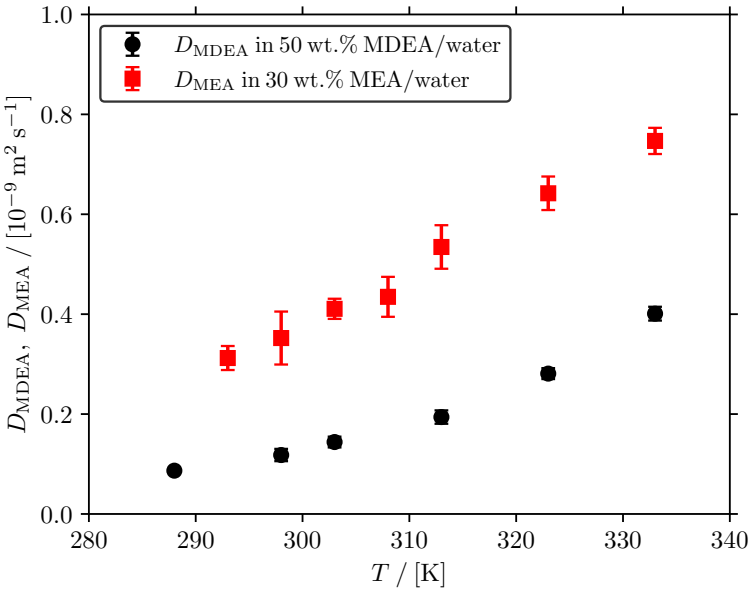

Figure S6: Comparison between the computed self-diffusities of MDEA D_{MDEA} in 50 wt% MDEA/water solution and D_{MEA} in 30 wt.% MEA/water solution [13] as a function of temperature at 1 bar. The self-diffusivities are corrected for finite-size effects using Eq. 1 of the main text. The point charges of MDEA and MEA [13] are scaled by 0.9 and 0.8, respectively. We compare the values of D_{MDEA} in a 50 wt% MDEA/water solution and the values of D_{MEA} in a 30 wt.% MEA/water solution because MDEA and MEA have similar mole fractions in these solutions ($X_{\mathrm{MDEA}} = 0.13$ in 50 wt.% MDEA/water solutions and $X_{\mathrm{MEA}} = 0.11$ in 30 wt.% MEA/water solutions).

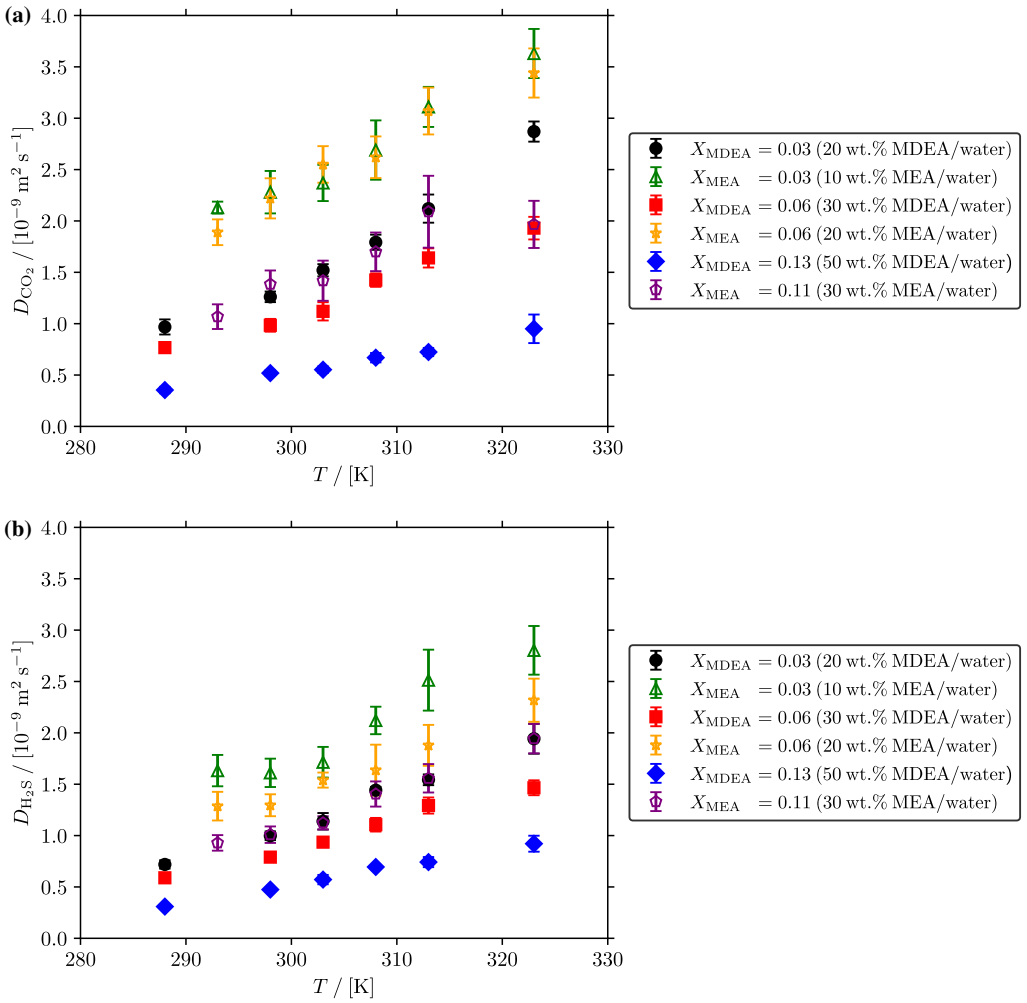

Figure S7: Comparison of (a) the self-diffusities of CO_2 D_{CO_2} and (b) the self-diffusities of H_2S D_{H_2S} in aqueous MDEA (this study) and MEA [13] solutions as a function of temperature at 1 bar. The self-diffusivities are corrected for finite-size effects using Eq. 1 of the main text. The point charges of MDEA and MEA [13] are scaled by 0.9 and 0.8, respectively. Note that due to the difference in the molar weights of MDEA and MEA, different weight percentages of MDEA and MEA can correspond to a similar molar fraction. For example, $X_{MDEA} = 0.03$ in 20 wt.% MDEA/water solutions while $X_{MEA} = 0.03$ in 10 wt.% MDEA/water solutions.

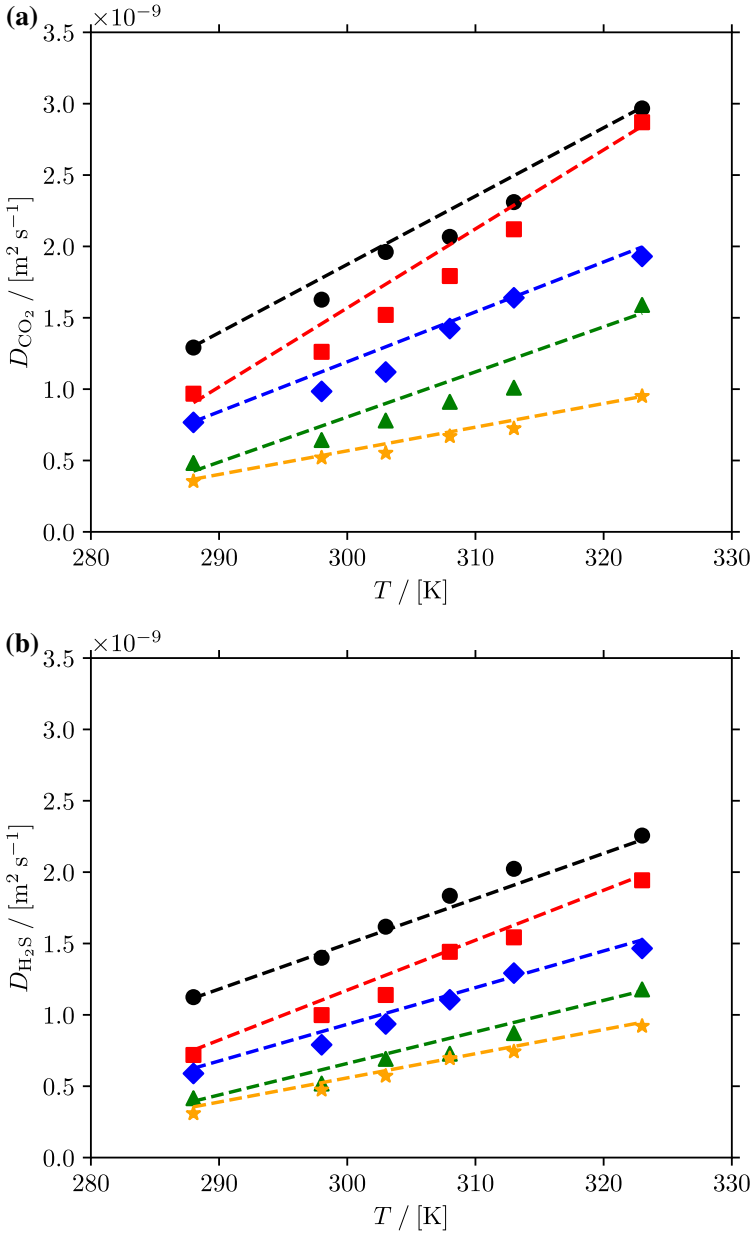

Figure S8: Computed values of (a) the self-diffusities of CO_2 D_{CO_2} and (b) the self-diffusities of H_2S D_{H_2S} as a function of temperature and MDEA concentration in the solution at 1 bar. The self-diffusivities are corrected for finite-size effects using Eq. 1 of the main text. The point charges of MDEA are scaled by 0.9. The dashed lines represent the fits to the Arrhenius equation. The color code follows that of Fig. S5.

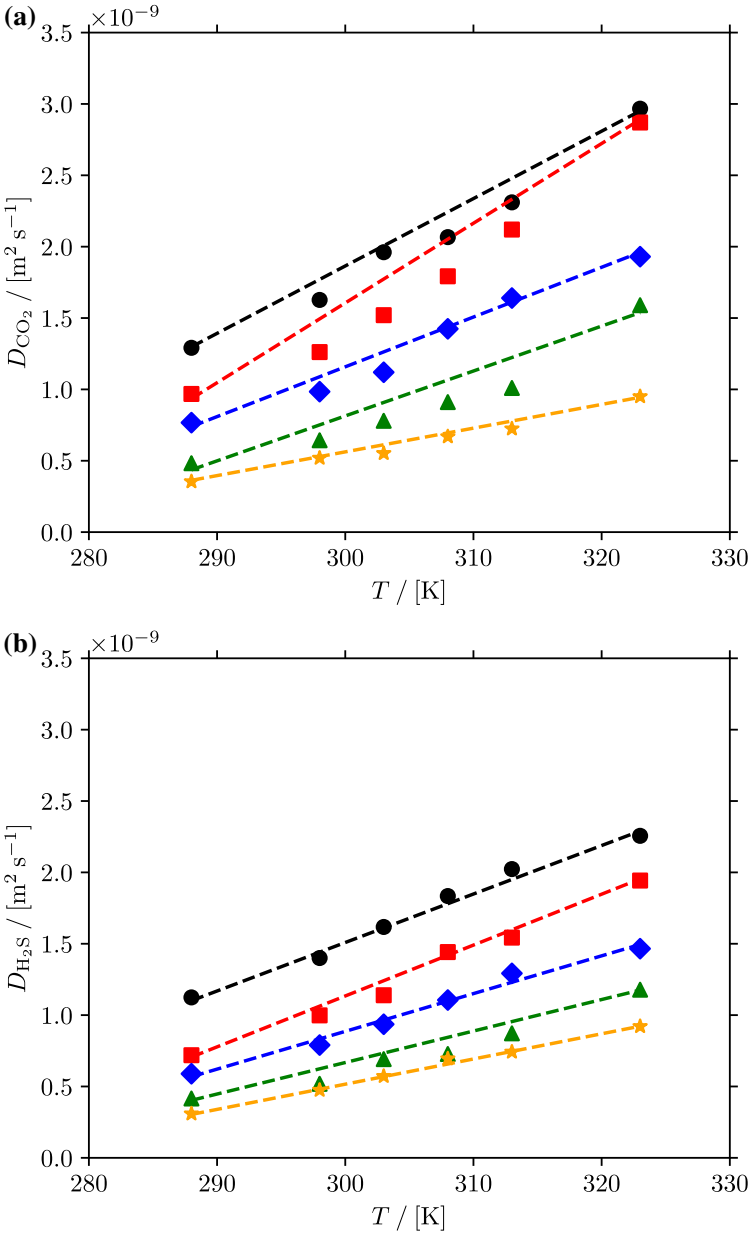

Figure S9: Computed values of (a) the self-diffusities of CO_2 D_{CO_2} and (b) the self-diffusities of H_2S D_{H_2S} as a function of temperature and MDEA concentration in the solution at 1 bar. The self-diffusivities are corrected for finite-size effects using Eq. 1 of the main text. The point charges of MDEA and MEA [13] are scaled by 0.9 and 0.8, respectively. The dashed lines represent the fits to the Speedy-Angell power equation [5]. The color code follows that of Fig. S5.

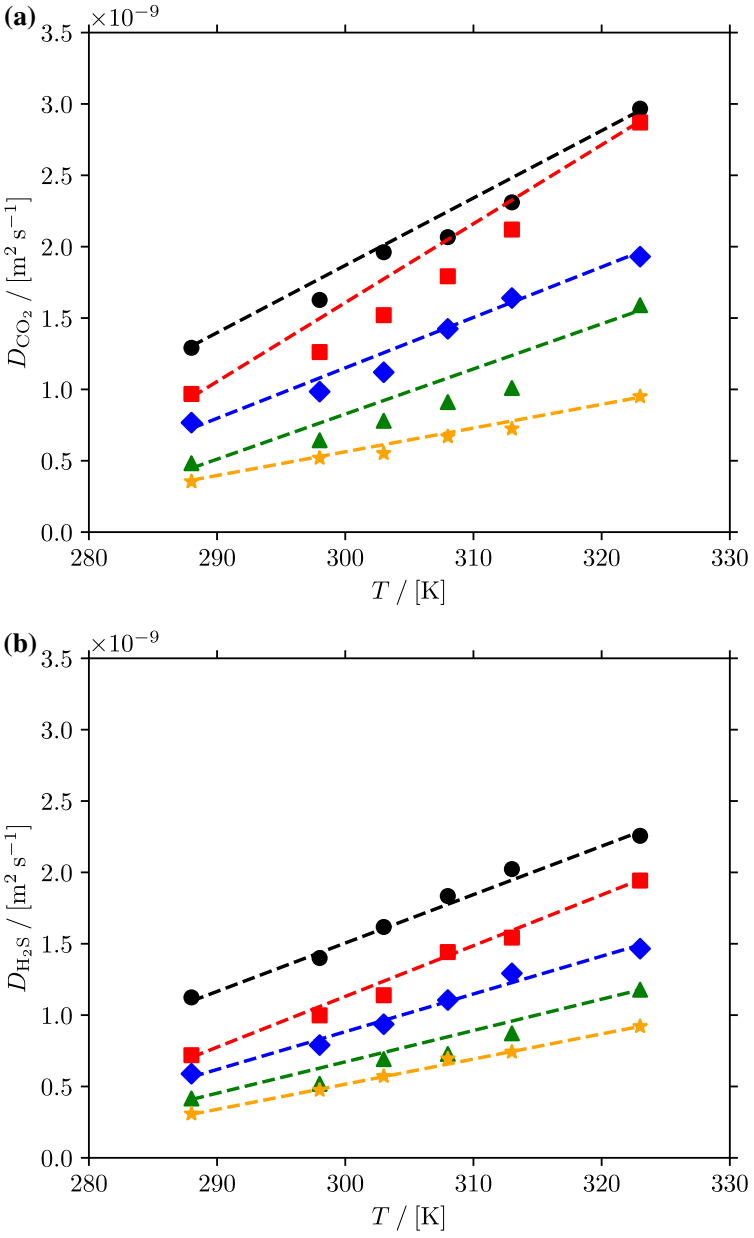

Figure S10: Computed values of (a) the self-diffusities of CO_2 D_{CO_2} and (b) the self-diffusities of H_2S D_{H_2S} as a function of temperature and MDEA concentration in the solution at 1 bar. The self-diffusivities are corrected for finite-size effects using Eq. 1 of the main text. The point charges of MDEA and MEA [13] are scaled by 0.9 and 0.8, respectively. The dashed lines represent the fits to the VTF equation [6]. The color code follows that of Fig. S5.

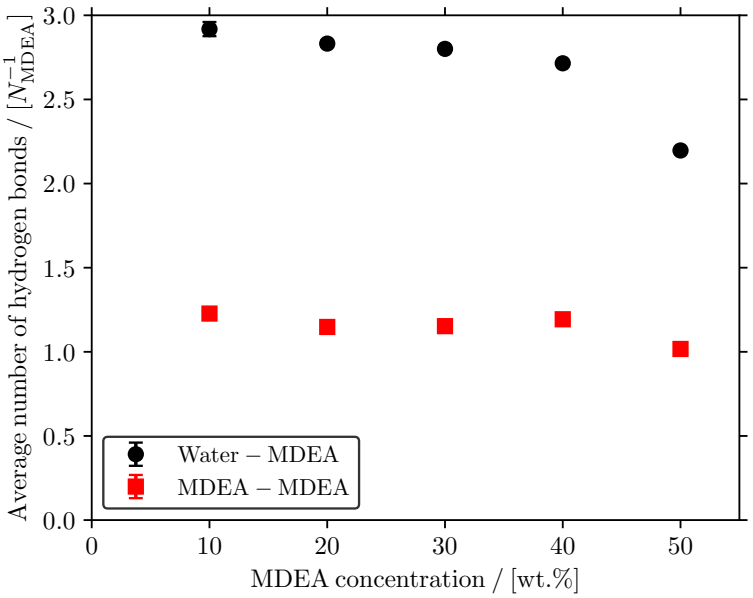

Figure S11: Average number of hydrogen bonds per MDEA molecule between water-MDEA and MDEA-MDEA pairs as a function of MDEA concentration in the solution at 313 K and 1 bar. Average number of hydrogen bonds are computed using VMD Hydrogen Bonds plugin [14] with a cutoff distance of 3.5 Å and a cutoff angle of 30° [15]. 2000 simulation snapshots are used to compute average number of hydrogen bonds.

References

[1] H. A. Al-Ghawas, D. P. Hagewiesche, G. Ruiz-Ibanez, O. C. Sandall, Physicochemical properties important for carbon dioxide absorption in aqueous methyldiethanolamine, Journal of Chemical and Engineering Data 34 (1989) 385–391.

[2] N. Haimour, O. C. Sandall, Molecular diffusivity of hydrogen sulfide in water, Journal of Chemical and Engineering Data 29 (1984) 20–22.

[3] W. D. Cornell, P. Cieplak, C. I. Bayly, I. R. Gould, K. M. Merz, D. M. Ferguson, D. C. Spellmeyer, T. Fox, J. W. Caldwell, P. A. Kollman, A second generation force field for the simulation of proteins, nucleic acids, and organic molecules, Journal of the American Chemical Society 117 (1995) 5179–5197.

[4] G. A. Orozco, V. Lachet, C. Nieto-Draghi, A. D. MacKie, A transferable force field for primary, secondary, and tertiary alkanolamines, Journal of Chemical Theory and Computation 9 (2013) 2097–2103.

[5] R. J. Speedy, C. A. Angell, Isothermal compressibility of supercooled water and evidence for a thermodynamic singularity at -45°C, The Journal of Chemical Physics 65 (1976) 851–858.

[6] W. Lu, H. Guo, I. M. Chou, R. C. Burruss, L. Li, Determination of diffusion coefficients of carbon dioxide in water between 268 and 473 K in a high-pressure capillary optical cell with in situ raman spectroscopic measurements, Geochimica et Cosmochimica Acta 115 (2013) 183–204.

[7] J. J. Potoff, J. I. Siepmann, Vapor–liquid equilibria of mixtures containing alkanes, carbon dioxide, and nitrogen, AIChE Journal 47 (2001) 1676–1682.

[8] M. S. Shah, M. Tsapatsis, J. I. Siepmann, Development of the transferable potentials for phase equilibria model for hydrogen sulfide, Journal of Physical Chemistry B 119 (2015) 7041–7052.

[9] J. L. F. Abascal, C. Vega, A general purpose model for the condensed phases of water: TIP4P/2005, Journal of Chemical Physics 123 (2005) 234505.

[10] G. A. Orozco, I. G. Economou, A. Z. Panagiotopoulos, Optimization of intermolecular potential parameters for the CO_2/H_2O mixture, Journal of Physical Chemistry B 118 (2014) 11504–11511.

[11] W. L. Jorgensen, D. S. Maxwell, J. Tirado-Rives, Development and testing of the OPLS all-atom force field on conformational energetics and properties of organic liquids, Journal of the American Chemical Society 118 (1996) 11225–11236.

[12] R. C. Rizzo, W. L. Jorgensen, OPLS all-atom model for amines: Resolution of the amine hydration problem, Journal of the American Chemical Society 121 (1999) 4827–4836.

[13] H. M. Polat, F. de Meyer, C. Houriez, C. Coquelet, O. A. Moultos, T. J. H. Vlugt, Transport properties of mixtures of acid gases with aqueous monoethanolamine solutions: A molecular dynamics study, Fluid Phase Equilibria 564 (2023) 113587.

[14] W. Humphrey, A. Dalke, K. Schulten, VMD – Visual Molecular Dynamics, Journal of Molecular Graphics 14 (1996) 33–38.

[15] A. Luzar, D. Chandler, Effect of environment on hydrogen bond dynamics in liquid water, Physical Review Letters 76 (1996) 928–931.